



**HAL**  
open science

## ***β*4-Nicotinic Receptors Are Critically Involved in Reward-Related Behaviors and Self-Regulation of Nicotine Reinforcement**

Marianne Husson, Lauriane Harrington, Léa Tochon, Yoon H Cho, Inés Ibañez-Tallon, Uwe Maskos, Vincent David

► **To cite this version:**

Marianne Husson, Lauriane Harrington, Léa Tochon, Yoon H Cho, Inés Ibañez-Tallon, et al.. *β*4-Nicotinic Receptors Are Critically Involved in Reward-Related Behaviors and Self-Regulation of Nicotine Reinforcement. *Journal of Neuroscience*, 2020, 40 (17), pp.3465-3477. 10.1523/JNEUROSCI.0356-19.2020 . hal-02888323

**HAL Id: hal-02888323**

**<https://hal.science/hal-02888323v1>**

Submitted on 3 Jul 2020



**HAL** is a multi-disciplinary open access archive for the deposit and dissemination of scientific research documents, whether they are published or not. The documents may come from teaching and research institutions in France or abroad, or from public or private research centers.

L'archive ouverte pluridisciplinaire **HAL**, est destinée au dépôt et à la diffusion de documents scientifiques de niveau recherche, publiés ou non, émanant des établissements d'enseignement et de recherche français ou étrangers, des laboratoires publics ou privés.



Distributed under a Creative Commons Attribution 4.0 International License

# $\beta$ 4-Nicotinic Receptors Are Critically Involved in Reward-Related Behaviors and Self-Regulation of Nicotine Reinforcement

Marianne Husson,<sup>1,2\*</sup> Lauriane Harrington,<sup>3,4\*</sup> Léa Tochon,<sup>1,2</sup> Yoon Cho,<sup>1,2</sup>  Inés Ibañez-Tallon,<sup>5</sup> Uwe Maskos,<sup>3†</sup> and  Vincent David<sup>1,2†</sup>

<sup>1</sup>Université de Bordeaux, Institut de Neurosciences Cognitives et Intégratives d'Aquitaine, 33615 Pessac, France, <sup>2</sup>Institut de Neurosciences Cognitives et Intégratives d'Aquitaine, Centre National de la Recherche Scientifique (CNRS) Unité Mixte de Recherche (UMR) 5287, 33615 Pessac, France, <sup>3</sup>Département de Neurosciences, Institut Pasteur, Unité Neurobiologie Intégrative des Systèmes Cholinergiques, 75724 Paris, France, <sup>4</sup>Sorbonne Université, Collège Doctoral, 75005 Paris, France, and <sup>5</sup>Laboratory of Molecular Biology, the Rockefeller University, New York, New York 10065

Nicotine addiction, through smoking, is the principal cause of preventable mortality worldwide. Human genome-wide association studies have linked polymorphisms in the *CHRNA5-CHRNA3-CHRN4* gene cluster, coding for the  $\alpha$ 5,  $\alpha$ 3, and  $\beta$ 4 nicotinic acetylcholine receptor (nAChR) subunits, to nicotine addiction.  $\beta$ 4\*nAChRs have been implicated in nicotine withdrawal, aversion, and reinforcement. Here we show that  $\beta$ 4\*nAChRs also are involved in non-nicotine-mediated responses that may predispose to addiction-related behaviors.  $\beta$ 4 knock-out (KO) male mice show increased novelty-induced locomotor activity, lower baseline anxiety, and motivational deficits in operant conditioning for palatable food rewards and in reward-based Go/No-go tasks. To further explore reward deficits we used intracranial self-administration (ICSA) by directly injecting nicotine into the ventral tegmental area (VTA) in mice. We found that, at low nicotine doses,  $\beta$ 4KO self-administer less than wild-type (WT) mice. Conversely, at high nicotine doses, this was reversed and  $\beta$ 4KO self-administered more than WT mice, whereas  $\beta$ 4-overexpressing mice avoided nicotine injections. Viral expression of  $\beta$ 4 subunits in medial habenula (MHb), interpeduncular nucleus (IPN), and VTA of  $\beta$ 4KO mice revealed dose- and region-dependent differences:  $\beta$ 4\*nAChRs in the VTA potentiated nicotine-mediated rewarding effects at all doses, whereas  $\beta$ 4\*nAChRs in the MHb-IPN pathway, limited VTA-ICSA at high nicotine doses. Together, our findings indicate that the lack of functional  $\beta$ 4\*nAChRs result in deficits in reward sensitivity including increased ICSA at high doses of nicotine that is restored by re-expression of  $\beta$ 4\*nAChRs in the MHb-IPN. These data indicate that  $\beta$ 4 is a critical modulator of reward-related behaviors.

**Key words:** addiction; habenula; interpeduncular nucleus; nicotine; nicotinic receptors; reward

## Significance Statement

Human genetic studies have provided strong evidence for a relationship between variants in the *CHRNA5-CHRNA3-CHRN4* gene cluster and nicotine addiction. Yet, little is known about the role of  $\beta$ 4 nicotinic acetylcholine receptor (nAChR) subunit encoded by this cluster. We investigated the implication of  $\beta$ 4\*nAChRs in anxiety-, food reward- and nicotine reward-related behaviors. Deletion of the  $\beta$ 4 subunit gene resulted in an addiction-related phenotype characterized by low anxiety, high novelty-induced response, lack of sensitivity to palatable food rewards and increased intracranial nicotine self-administration at high doses. Lentiviral vector-induced re-expression of the  $\beta$ 4 subunit into either the MHb or IPN restored a “stop” signal on nicotine self-administration. These results suggest that  $\beta$ 4\*nAChRs provide a promising novel drug target for smoking cessation.

## Introduction

Tobacco consumption is the primary cause of preventable mortality and morbidity worldwide, with an estimated 6 million

deaths per year (WHO, 2011). Self-motivated cessation rates are very low, with only 3–10% of smokers able to abstain for >12 months, even with pharmacological cessation aids (Hartmann-

Received Feb. 4, 2019; revised Jan. 30, 2020; accepted Feb. 18, 2020.

Author contributions: U.M. and V.D. designed research; M.H., L.H., Y.C., L.T., I.I.-T., and V.D. performed research; M.H., L.H., and V.D. analyzed data; M.H. and V.D. wrote the paper.

\*M.H. and L.H. contributed equally to this work.

†U.M. and V.D. equally supervised this work.

Boyce et al., 2013). Therefore, it remains essential to further investigate the neurobiological mechanisms involved in nicotine dependence and its action on nicotinic acetylcholine receptors (nAChRs). nAChRs are ligand-gated cation channels, activated by the endogenous neurotransmitter acetylcholine (ACh), that assemble into homo- or hetero-pentamers of  $\alpha$  ( $\alpha 2$ – $\alpha 7$  and  $\alpha 9$ – $\alpha 10$ ) and  $\beta$  ( $\beta 2$ – $\beta 4$ ) subunits (McGehee and Role, 1995; Gotti et al., 2009). Although the roles of widely expressed nAChR subtypes, like  $\beta 2$ -containing ( $\beta 2^*$ ) and  $\alpha 7^*$  nAChRs have been largely investigated this past decade (Changeux, 2010; Picciotto and Mineur, 2014), much less work has been conducted on  $\alpha 5^*$ ,  $\alpha 3^*$ , and  $\beta 4^*$  nAChRs encoded by the *CHRNA5-CHRNA3-CHRNA4* gene cluster, in which genetic variants have been linked to high predisposition to nicotine dependence in humans (Amos et al., 2008; Thorgeirsson et al., 2008; Weiss et al., 2008; Saccone et al., 2009).

$\beta 4^*$ nAChRs are almost exclusively expressed in the medial habenula (MHb), its efferent target the interpeduncular nucleus (IPN), autonomic ganglia, and at low levels in the ventral tegmental area (VTA; Zoli et al., 1995; Klink et al., 2001; Azam et al., 2002; Salas et al., 2004a).  $\beta 4^*$ nAChRs are involved in nicotine-induced MHb-IPN activity (Shih et al., 2014) and are the sole nAChR subtype allowing stimulation of ACh release in the IPN (Grady et al., 2009; Beiranvand et al., 2014). The MHb-IPN axis is a key player in nicotine withdrawal and consumption, implicating both  $\alpha 5$  and  $\beta 4$  subunits (Salas et al., 2004a,b, 2009; Velasquez et al., 2014). Knock-out mice (KO) of  $\alpha 5$  and  $\beta 4$  nAChRs show similarly reduced nicotine withdrawal syndrome and anxiety-like response (Jackson et al., 2008; Salas et al., 2009). Transgenic mice overexpressing  $\beta 4^*$ nAChRs (“Tabac”) show increased sensitivity to the aversive properties of nicotine and consequently decreased nicotine drinking behavior and strong conditioned place aversion at low nicotine doses that have no effects in wild-type (WT; Frahm et al., 2011). The  $\beta 4$  subunit is implicated also in nicotine positive reinforcement. Mice overexpressing the entire gene cluster show increased sensitivity to acute nicotine, facilitated self-administration, and MHb activation, but reduced nicotine-induced activation of the VTA (Gallego et al., 2012). Intravenous self-administration (IVSA) of nicotine is reduced in  $\beta 4$ KO mice; yet nicotine-induced mesolimbic dopamine (DA) release and sensitivity of VTA DA neurons to nicotine are increased (Harrington et al., 2016). Also, intrahabenular injection of the  $\alpha 3\beta 4$  receptor antagonist 18-methoxycoronaridine blocked mesolimbic DA release (Glick et al., 2006; McCallum et al., 2012).

Given these contrasting data, we further explored the role of  $\beta 4^*$ nAChRs in anxiety-related behaviors, sensitivity to palatable food rewards, and nicotine’s reinforcing properties using intracranial self-administration (ICSA) in the VTA (Maskos et al.,

2005; Besson et al., 2006; David et al., 2006; Exley et al., 2011; Tolu et al., 2013) in WT,  $\beta 4$ KO,  $\beta 4$ -overexpressing Tabac mice, and KO mice re-expressing  $\beta 4$  in either the VTA or the MHb-IPN pathway.

## Methods

### Animals and ethical statement

All surgical and experimental procedures were conducted in accordance with the European Community’s Council Directive of 24 November 1986 (86/609/EEC) and a local ethics committee [Comité d’Éthique en Expérimentation Animale de l’Université de Bordeaux (CEE50), and Comité d’Éthique en Expérimentation Animale de l’Institut Pasteur, 2013-0097]. We used WT (C57BL/6J strain),  $\beta 4^*$ -nAChR KO mice ( $\beta 4^{-/-}$  mice), bacterial artificial chromosome transgenic mice overexpressing the  $\beta 4$  subunit (Tabac; Frahm et al., 2011). All were males and were raised at Charles River Laboratories, submitted to the same life conditions. Mice were housed with *ad libitum* access to food and water in a temperature-controlled room (23°C) with a 12 h light/dark cycle (lights on at 8:00 A.M.). Following surgery for VTA-ICSA preparation, mice were housed individually. Mice were aged 2–3 months for lentivirus injections and 3–4 months (25–30 g) at the beginning of the behavioral experiments.

### Locomotor activity

Spontaneous horizontal locomotor activity of  $\beta 4$ KO and WT mice in a new environment was recorded for 14 h using automated locomotor boxes (Actimeter apparatus, Imetronic). The first 2 h were recorded during the end of the light phase (18:00–20:00), the remaining 12 h corresponding to the dark phase of the cycle.

### Elevated plus maze

Anxiety-like behavior was assessed in the elevated plus maze (EPM). The apparatus was composed of gray PVC and consisted of four arms. Each arm was 30 cm long, 7 cm wide, and 60 cm above the ground. The four arms were joined at the center by a 7 cm square platform. Two opposite arms of the plus maze were “closed” by 24-cm-high sidewalls but open on the top, and the other arms did not have sidewalls. Light intensity in open arms was 70 lx. At the beginning of each test, the mouse was placed in the center of the maze in a cylinder (7 cm in diameter, 17 cm high) for 30 s. Then, the cylinder was removed and the animal was allowed to explore all arms of the maze freely for 8 min. An entry was counted when the mouse entered an arm with all 4 feet. Four independent groups of WT ( $n = 15$ ) and KO ( $n = 16$ ) mice received an intraperitoneal injection of either NaCl or nicotine 0.2 mg/kg, 10 min before testing. The number of entries and latency to enter open and closed arms were measured, as well as the time spent and the distance traveled in open and closed arms. Data were expressed as the open/total entry ratio, percentage time and percentage distance in open arms.

### Operant conditioning for a palatable food reward

The apparatus used were five rectangular operant chambers (28 cm L, 18 cm W  $\times$  18 cm H) constructed of black PVC. Briefly, each chamber was equipped with a total of 11 nose-poke holes (13 mm diameter) distributed over three of its inner walls. Three of these (Holes 1–3 from left to right) were placed in a horizontal row on the left wall. Five holes forming an X (Holes 4–8 from left to right, and top to bottom) were placed on the front wall. And finally, the last three holes were spaced in a

This work was supported by FP7 ERANET program (NICO-GENE), the Institut Pasteur, Center National de la Recherche Scientifique CNRS UMR 3571 (U.M.) and CNRS UMR 5287 (V.D.) and the Agence Nationale pour la Recherche (ANR-10-BLAN-1437, project “NICOSTOP”), the French National Cancer Institute (INCA-CANCERPOLE-TABAC-01-16022), the EC FP7 Grant agreement “NeuroCypres” project, Fondation EDF, the Fondation des Treilles, and the Foundation for Medical Research FMR. U.M. is a member of the Laboratory of Excellence, Bio-Psy Labex; as such this work was supported by French state funds managed by the Agence Nationale pour la Recherche (ANR) within the Investissements d’Avenir program under reference ANR-11-IDEX-0004-02. The team of U.M. is part of the Ecole des Neurosciences de Paris Ile-de-France Network. Work in New York was supported by National Institute on Drug Abuse Grant P30DA035756. We thank Stéphanie Pons for constant support and discussions, and Martine Soudant for technical assistance.

The authors declare no competing financial interests.

Correspondence should be addressed to Vincent David at [vincent.david@u-bordeaux.fr](mailto:vincent.david@u-bordeaux.fr).

<https://doi.org/10.1523/JNEUROSCI.0356-19.2020>

Copyright © 2020 the authors

vertical column on the right wall (Holes 9–11 from top to bottom). Each nose-poke hole was equipped with a light emitting diode for its illumination, and a pair of photobeam cells for the detection of the mouse nose poking into that hole. On the floor near the rear wall was located a liquid dispenser delivering liquid reinforcements via an electro-valve release mechanism. They were trained for nose-poking using a continuous reinforcement schedule, that is, any nose-poke resulted in the immediate delivery of 7  $\mu$ l of 2% sucrose whole-milk reward. C57BL/6J Mice typically emit  $\sim$ 50 reinforced responses after five to six daily 20 min sessions (Cho and Jeantet, 2010).

### Reward-guided Go/No-go discrimination procedure

Mice were first familiarized with crisp reward as small, 5mm<sup>2</sup> pieces freely available in their home cage during the 3 d preceding the beginning of experiments. The first session consisted of a 10 min free exploration of the Y-maze. Starting on Day 2, each daily session consisted in four consecutive trials, two of which were reinforced (R+) with the delivery of one 5mm<sup>2</sup> piece of crisp, whereas the other 2 were not (R-). Small pieces (5 mm<sup>2</sup>) of naturally flavored crisps (Vico) were chosen as food reward after previous studies showing that motivation to learn a Y-maze discrimination task was obtained with a very low level of deprivation (Baudonnat et al., 2011). Therefore mice were deprived to reach 95% of their *ad libitum* body weight 3 d before the beginning of experiments. For each trial, the door of only one arm (which could be reinforced or not) was open. The reinforced arm (R+) remained constant through training, but the presentation order changed randomly from one session to another. Latency to enter arm R+ and R- are measured. Discrimination performance was assessed using the ratio between R+ and R- latencies. Successful discrimination was obtained when the mean R+ latency is significantly shorter than R- latency for three consecutive sessions (R+/R- < 1). C57BL/6J mice typically reached this criterion after six sessions.

### Intra-VTA nicotine self-administration

Nicotine reinforcement was assessed using a previously described mouse model of VTA-ICSA based on choice behavior between a nicotine-reinforced and a neutral arm in a Y-maze discrimination task, and detecting both rewarding and aversive properties (Besson et al., 2006; David et al., 2006; Exley et al., 2011; Tolu et al., 2013). This task was previously shown to be well adapted to detect reward deficits in mutant mice, and allows excellent temporal and spatial, region-specific delivery of nicotine for targeting brain structures such as the VTA.

The present experiments were conducted in a gray Plexiglas Y-maze, the arms of which were separated by an angle of 90°. The stem and the arms were 31 cm long and 12 cm high. The starting box (14  $\times$  8 cm) was separated from the stem by a sliding door. Each arm had a sliding door at its entrance and a photoelectric cell 6 cm from its end. Mice were implanted unilaterally into the posterior VTA, using the coordinates of lentiviral injections. Before each experimental session, a stainless-steel injection cannula (outer diameter 0.229 mm, inner diameter 0.127 mm) was inserted into the VTA and held in a fixed position by a small connector. The tip of the injection cannula projected beyond the guide-cannula by 1.5 mm. It was connected by flexible polyethylene tubing to the microinjection system, which housed a 5  $\mu$ l Hamilton syringe containing a solution of nicotine in artificial CSF (aCSF; microperfusion fluid; Phymep). The first session consisted of a 10 min free exploration of the Y-maze. During the second session, mice were habituated to being connected to the

self-injection system (no injection). In subsequent sessions, the interruption of photocell beams by the mouse entering the reinforced arm of the Y-maze triggered an intra-VTA injection of nicotine which lasted 4 s. Because the photo beams were located only 6 cm from the end of each arm, the mouse had to enter an arm completely to end a trial. Therefore, partial entrance into the arm did not count as a choice. Entering the non-reinforced arm produced no injection, and entering either arm terminated the trial. The animal's movements were detected using an optical system and transmitted to a computer, which rotated the injector in the same direction, thus avoiding twisting. Intracranial injections were conducted using an automated computer-controlled apparatus for precise and reproducible delivery of nicotine (YAA, Imetronic). Following a 25 s enclosure in the target arm, the mouse is guided back to the start arm to end the trial. Mice were submitted to 10 trials per session with a 1 min intertrial interval, and one session per day. A maximum of 10 injections could be obtained by each mouse per daily session (chance level: 50%). The number of triggered injections within the nicotine-reinforced arm per daily session (number of self-administrations) and the self-injection latency for each subject were automatically recorded ("YAA" software, Imetronic). The mean of one daily session provided one graph plot. The nicotine-associated arm was assigned randomly and alternatively to each mouse, and remained constant through the experiments. The experimenter was blind to the genotypes.

### Drugs

(-)-Nicotine hydrogen ditartrate salt (Sigma-Aldrich) was dissolved in aCSF (Phymep) and the pH adjusted to 6.9–7.4 using NaOH. Doses used were 0.4, 2, 4, 24, and 48 mM nicotine (salt concentration), delivered intracranially as 50 nl injections (10, 50, 100, 600, and 1200 ng/50 nl nicotine).

### Lentiviral expression vector

A lentiviral vector was generated based on the work by Harrington et al. (2016). The construct (Fig. 1A), contains  $\beta 4$  mouse cDNA and green fluorescent protein (GFP) genetic sequences, whose expression is driven by the phosphoglycerate kinase (PGK) promoter (PGK- $\beta 4$ ). The  $\beta 4$ -containing lentiviral construct was obtained by subcloning strategies. The control lentiviral vector (LV) induces GFP expression only (PGK-GFP).

### Stereotaxic surgical procedure for LV delivery

WT and KO mice were anesthetized by intraperitoneal ketamine and xylazine (5:1; 0.10 ml/10 g) and placed with the skull exposed in a stereotaxic frame (Stoelting). Surgery was conducted under aseptic conditions. The VTA was targeted as previously described (Tolu et al., 2013), and the MHb and IPN targeted as recently published (Harrington et al., 2016). LVs were injected bilaterally into the VTA at anteroposterior  $-3.40$  mm from bregma, lateral  $\pm 0.5$  mm and ventral  $-4.4$  mm from the surface. The MHb was targeted from bregma and skull surface at: anterior  $-1.90$  mm, lateral  $\pm 1.25$  mm and ventral  $-2.40$  mm (Paxinos and Franklin, 2001). Injections were conducted using pulled glass pipettes at an angle of  $\pm 20^\circ$ . Two 0.5  $\mu$ l volumes of LV were delivered bilaterally at 0.2  $\mu$ l/min (PGK- $\beta 4$  300 ng/ $\mu$ l, PGK-GFP 75 ng/ $\mu$ l p24 protein). The IPN was targeted at anterior:  $-3.60$  mm, lateral:  $\pm 1.60$  mm, and ventral:  $-4.50$  mm from bregma and skull surface at an angle of  $20^\circ$ . A metal 35-gauge needle was used to deliver a single injection of 2  $\mu$ l LV to the central region of the IPN (PGK- $\beta 4$  75 ng/ $\mu$ l, PGK-GFP 25 ng/ $\mu$ l p24 protein). LV-injected mice underwent behavioral

testing 5 weeks postinjection. LV-injected mice were euthanized 2–4 weeks post-injection for immunohistological analysis (Fig. 1B).

### Quantification of $\beta 4^*$ nAChR expression

Mice were euthanized by CO<sub>2</sub>. The brains were dissected and frozen at  $-80^{\circ}\text{C}$ . Twenty micrometer coronal sections were obtained using a cryostat at  $-20^{\circ}\text{C}$  and thaw mounted onto microscope slides (Menzel Glaser SuperFrost Plus). Radioligand binding was performed as described previously (Harrington et al., 2016), using the  $\beta 2^*$ -specific 5-Iodo-A-85380 dihydrochloride (25 nM, A85380, Tocris Bioscience) as the cold ligand. Total I125-epibatidine (220 pM, 2200 Ci/mmol-specific activity, PerkinElmer) *in situ* binding indicates localization of heteromeric nAChRs. A85380-resistant I125-epibatidine binding indicates localization of putatively  $\beta 4^*$ nAChRs, because I125-epibatidine is displaced from  $\beta 2^*$ nAChR sites. Following the binding procedure, slides were exposed to a Biomax MR film (Kodak) for 16 h. Developed films were scanned at 1600 dpi for analysis using Fiji software. The mean inverse luminosity of three background points was subtracted from the measured inverse luminosity of autoradiographic puncta. Data were normalized to WT controls. Autoradiographic analysis of brains following nicotine VTA-ICSA revealed the heterogeneous nature of  $\beta 4$  re-expression in the MHB among individuals. As in the study of Harrington et al. (2016), mice with a low level of  $\beta 4$  subunit re-expression relative to WT according to radioligand binding (mean 28%), exhibited a KO-like response to nicotine. Therefore, subjects with this low level of re-expression (<30%) were removed from the current study as well. We observed no A8530-resistant I125-epibatidine binding in the LHb. Radioligand binding and immunofluorescence testing cannot be done on the same mouse brain (due to technical considerations), however, residual GFP expression was occasionally noted in the LHb (Fig. 1B). Yet LV-induced  $\beta 4$  re-expression was never observed in the LHb likely because there were no  $\alpha 3$  subunits, which are required for  $\beta 4$  subunit assembly. Therefore, we anticipate no impact on the present findings.

### Immunohistofluorescence

Deeply anesthetized WT and KO mice (ketamine:xylazine solution, i.p.) were intracardially perfused with PBS and 4% paraformaldehyde. Sixty-micrometer-thick coronal brain sections were obtained using a vibratome (Leica Microsystems). Sections were incubated in 10% normal horse serum (NHS) plus 0.2% Triton X-100 in PBS for 3 h. Proceeding incubations were conducted in 2% NHS and 0.04% Triton X-100. Primary antibodies used: rabbit anti-GFP (Life Technology), sheep anti-tyrosine hydroxylase (Millipore), goat anti-choline acetyl transferase (Chemi-Con) at 1:500 dilution, overnight,  $4^{\circ}\text{C}$ . Corresponding secondary antibodies (donkey anti-rabbit AlexaFluor-488, Abcam; donkey anti-sheep Cy5, Jackson; donkey anti-goat AlexaFluor-546, Life Technologies) were used for localization of primary antibodies at a 1:500 dilution for 4 h, room temperature. Images were obtained using a Zeiss fluorescent microscope.

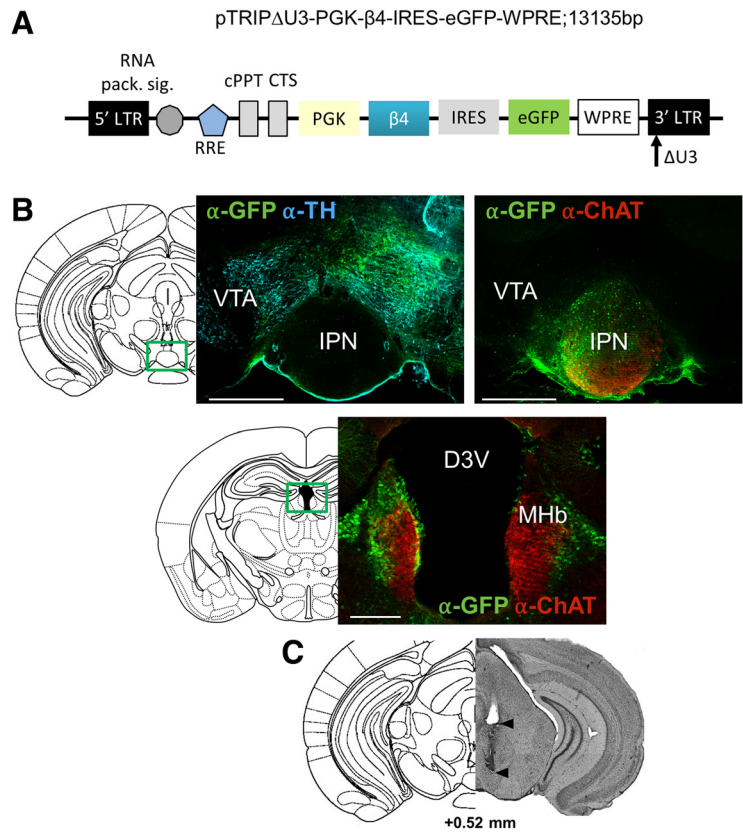


**Figure 1.** Validation of lentiviral transduction in the VTA, IPN, and MHB. **A**, LV contains  $\beta 4$  mouse cDNA and GFP genetic sequences, whose expression are driven by the PGK promoter. Control LV (PGK-GFP) was injected in WT and KO mice. LV for  $\beta 4^*$ nAChR expression (PGK- $\beta 4$ ) was injected in another group of KO, targeting the VTA, MHB, and IPN. Five weeks later, mice started nicotine VTA-ICSA. At the end of the last VTA-ICSA session, brains were removed for histologic control of stereotaxic implantation, control of LV-induced GFP expression (immunofluorescence) and determination of lentivector-introduced  $\beta 4$  expression (radioligand binding). **B**, Representative images of test ( $\beta 4$ -IRES-GFP) LV-induced GFP (green) expression in the VTA, IPN, and MHB in three different WT brains. Immunofluorescence was used to label GFP and tyrosine hydroxylase (TH; dopamine neuron marker), and choline acetyltransferase (ChAT; cholinergic neurons marker). Scale bar, 500  $\mu\text{m}$  (D3V: dorsal third ventricle). **C**, Photomicrograph of a thionine-stained coronal brain section (60  $\mu\text{m}$ ) through the guide-cannula track (top arrow) and the nicotine injection site in the VTA (bottom arrow). AP coordinate is relative to interaural line (Paxinos and Franklin, 2001).

### Histologic control

Implantation of nicotine-injection cannulas and tissue damage around the VTA injection site were verified for all subjects included in statistical analyses, using photomicrographs of thionine-stained frontal brain sections (60  $\mu\text{m}$ ) through the guide-cannula tracks. Out of 94 implanted animals, 7 were removed from the experiments for misplacement or blood clotting. A representative example of correct implantation and tissue damage is provided in Figure 1C, there was no observable tissue alteration at the level of the targeted structure (VTA), which appeared virtually intact following repeated nicotine injections, independently of the mouse genotype or nicotine dose. Arrows show the tip of injection cannula (site of injection, low) or guide-cannula (high).

### Statistical analyses

For anxiety- and reward-related behavioral tasks, all parameters were tested using two-way ANOVAs with “Genotype” as a between-subjects factor and “Session” as a within-subjects repeated measure. Nicotine self-administration was tested with two-way ANOVAs using the mean number of self-injections or total amount of nicotine intake (ng) as dependent variables,

Genotype as a between-subjects factor and Session as a within-subjects repeated measure. Significant main effects were explored by Newman–Keuls *post hoc* tests. Statistical analysis of A8380-resistant I125-epibatidine autoradiography was conducted with unpaired *t* test or one-way ANOVA followed by Tukey's *post hoc* tests. A significance level of  $p < 0.05$  was used for all statistical analyses.

## Results

### Effects of $\beta 4$ KO on anxiety-related behaviors

#### Novelty-induced locomotor activity

Novelty-induced activity and spontaneous locomotion during the dark phase were measured in  $\beta 4$ KO ( $n = 15$ ) and WT ( $n = 16$ ). Analyses of the first 2 h revealed that KO mice exhibited a significant increase in horizontal activity, which was more pronounced during the first 10 min and toward the end of the light-exposed session: Genotype Effect:  $F_{(1,29)} = 1.88$  ns; Time effect:  $F_{(12,348)} = 27.43$ ,  $p < 0.0001$ ; Genotype  $\times$  Time interaction:  $F_{(12,348)} = 2.02$ ,  $p = 0.02$  (Fig. 2A). In contrast, no difference was observed at any time between the two genotypes regarding spontaneous locomotor activity during the dark phase, which progressively decrease overnight similarly in both groups (Genotype Effect:  $F_{(1,12)} = 0.13$  ns; Time effect:  $F_{(71,2049)} = 25.51$ ,  $p < 0.0001$ ; Genotype  $\times$  Time interaction:  $F_{(71,2049)} = 0.92$  ns; Fig. 2B).

#### Elevated plus maze

We assessed anxiety level in  $\beta 4$ KO and WT littermates and the anxiolytic effects of nicotine (0.2 mg/kg, i.p.) using the EPM task. Vehicle-treated  $\beta 4$ KOs displayed an increase in all parameters i.e., the ratio of open arm/total entries (Fig. 2C), percentage time spent in the open arms (Fig. 2D) and percentage distance traveled in the open arms (Fig. 2E). The effects of a nicotine pre-injection (0.2 mg/kg, i.p.) 10 min before the task also strongly depended on the genotype: whereas all three parameters increased significantly in nicotine-treated WT subjects, no effects were observed in  $\beta 4$ KO mice. Two-way ANOVAs consistently revealed a significant effect of Genotype on open arm entries, percentage time spent and distance traveled in the open arms ( $F_{(1,23)} = 9.22$ ,  $p = 0.059$ ;  $F_{(1,23)} = 13.8$ ,  $p = 0.018$  and  $F_{(1,23)} = 24.3$ ,  $p = 0.0002$ , respectively); a main effect of nicotine treatment on both percentage time ( $F_{(1,23)} = 9.51$ ,  $p = 0.005$ ) and distance traveled in open arms ( $F_{(1,23)} = 9.00$ ,  $p = 0.005$ ), as well as a significant Genotype  $\times$  Nicotine interaction ( $F_{(1,23)} = 11.3$ ,  $p = 0.027$  and  $F_{(1,23)} = 8.00$ ,  $p = 0.009$ , respectively). Together, these data show a strong decrease in anxiety levels in  $\beta 4$ KO and a clear anxiolytic effect of nicotine in WT mice.

### Behavioral responses of $\beta 4$ KO mice in non-nicotine reward-dependent behaviors

#### Operant conditioning on a continuous-reinforcement schedule

Both  $\beta 4$ KO and WT mice progressively learned the task over the 12 acquisition sessions when using the 2% sucrose sweet milk. However, whereas most WT mice reached an asymptotic performance of 100 rewards by Session 9, KO mice exhibited a flat learning curve and earned half the number of rewards obtained by WT mice (Fig. 2F). These observations are supported by a two-way ANOVA revealing a strong Genotype effect ( $F_{(1,11)} = 26.23$ ,  $p = 0.0003$ ), a Session effect ( $F_{(11, 121)} = 57.77$ ,  $p < 0.0001$ ) and a Genotype  $\times$  Session interaction ( $F_{(11, 121)} = 29.61$ ,  $p < 0.0001$ ). When the sucrose concentration was increased to 10%, WT mice doubled the number of rewards earned by session (Fig. 2F). In contrast, KO mice were insensitive to variations in the sucrose

concentration, as attested by the number of rewards earned which remained around  $40 \pm 5/20$  min session despite changes in sucrose concentration (Genotype effect:  $F_{(1,11)} = 45.79$ ,  $p < 0.0001$ ).

#### Go/No-go discrimination procedure

We used another non-hippocampus-dependent task based on a successive discrimination procedure (Go/No-go) to further assess both motivational and executive processes (Marighetto et al., 1999). WT mice successfully learned to discriminate between R+ and R– arms of the Y-maze, exhibiting significant difference between R+ and R– latency by Session 4, reaching full discrimination criteria within 6 d (Fig. 2G). In contrast, KO mice did not exhibit any difference in the latency to reach R+ and R– over sessions (Fig. 2H). Strikingly, whereas impulsivity or executive deficits are typically associated with a non-discriminant decrease in R+ and R– latency,  $\beta 4$ KO displayed instead an undifferentiated increase of both R+ and R– latency. These observations are supported by a three-way ANOVA revealing a significant effect of Genotype:  $F_{(1,16)} = 26.60$ ,  $p = 0.005$ , a main effect of Reward (R+ vs R–):  $F_{(1,16)} = 21.05$ ,  $p = 0.017$ , a Session effect:  $F_{(5,90)} = 5.47$ ,  $p = 0.0001$  and a Genotype  $\times$  Reward interaction:  $F_{(5,90)} = 6.42$ ,  $p = 0.0119$ .

### VTA-ICSA responses in $\beta 4$ KO mice

#### $\beta 4^*$ nAChRs have inverse effects on nicotine reward as a function of dose

We first compared WT and KO mice using low doses of nicotine. Because no difference was observed with nicotine doses of 10 and 50 ng/50 nl in the number of nicotine self-injections, data obtained with these two doses were pooled (two-way ANOVA, Dose effect in WT:  $F_{(1,7)} = 3.53$  ns and Dose  $\times$  Session interaction,  $F_{(6,42)} = 1.12$  ns; in KO, Dose effect:  $F_{(1,9)} = 0.36$  ns, and Dose  $\times$  Session interaction:  $F_{(6,54)} = 1.93$  ns). KO mice self-administered less nicotine than WT over the acquisition phase (Genotype effect:  $F_{(1,18)} = 11.5$ ,  $p = 0.002$ ; Fig. 3A). At the optimally reinforcing dose of 100 ng, both WT and KO mice exhibited a significant and similar preference for the nicotine-reinforced arm of the Y-maze (Fig. 3B; ANOVA Session effect:  $F_{(6,78)} = 12.0$ ,  $p < 0.0001$ ).

We then investigated the effects of high doses (7 d at 600 ng followed by 7 d at 1200 ng/50 nl) in mutant strains expressing different levels of the  $\beta 4$  subunit: WT,  $\beta 4$ KO and  $\beta 4$  overexpressing Tabac mice. At 600 ng, KO mice exhibited a weak preference for the nicotine-reinforced arm, which remained stable across sessions with no significant difference between WT and KO groups (Fig. 3C). Conversely, Tabac mice exhibited a marked avoidance of nicotine, remaining below chance level over all sessions, leading to a significant Genotype effect (two-way ANOVA):  $F_{(2,23)} = 3.75$ ,  $p = 0.039$ ; no Session effect:  $F_{(6,138)} = 0.62$  ns; and no Genotype  $\times$  Session interaction:  $F_{(12,138)} = 0.60$  ns. Doubling the dose (600–1200 ng) enhanced genotype-dependent effects. Whereas nicotine VTA-ICSA further increased over sessions in KO mice, choice of the nicotine reinforced-arm remained at chance level in WTs, whereas Tabac mice displayed a strong avoidance (two-way ANOVA, Genotype effect:  $F_{(2,23)} = 9.47$ ,  $p = 0.001$ ; Session effect:  $F_{(6,138)} = 1.41$  ns; Genotype  $\times$  Session interaction:  $F_{(12,138)} = 1.38$  ns). *Post hoc* analysis confirmed that KO mice preferred the nicotine-reinforced arm, whereas Tabac mice preferred the non-reinforced arm compared with WT mice or chance (Fig. 3C). Analyses of nicotine intake were consistent with the number of self-administration events for each genotype. Indeed, the total amount of nicotine intake increased in WT in a dose-dependent manner, but significantly more in KO and conversely less in Tabac mice, leading to strong effects of Dose:  $F_{(1,46)} = 41.97$ ,

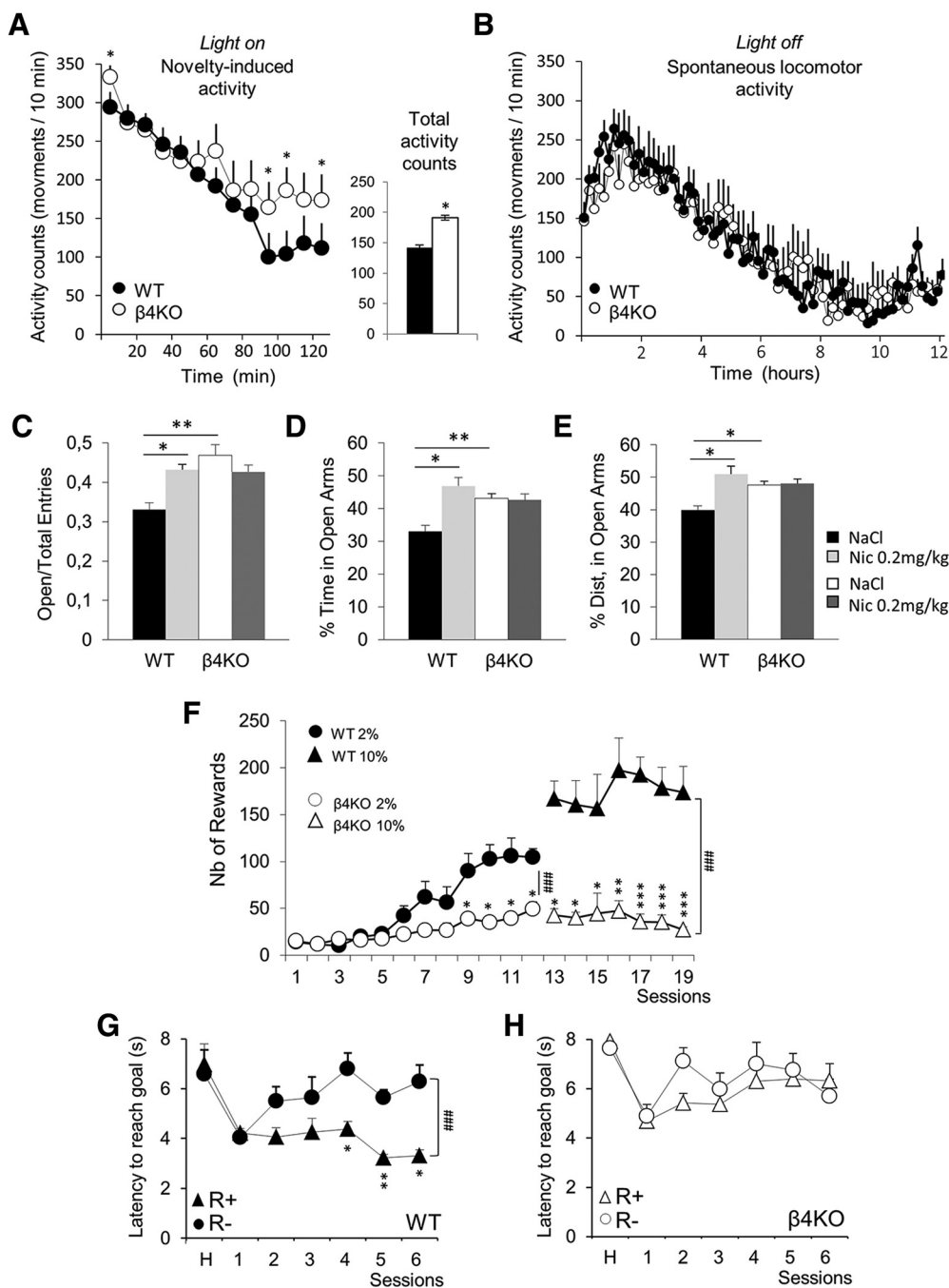


**Figure 2.** Anxiety-related and reward-dependent behaviors in  $\beta 4$ KO mice. **A, B**, Novelty-induced locomotor activity. Mean number ( $\pm$ SEM) of photobeam crosses during the first 2 h of the session corresponding to the last 2 h of the light cycle (**A**) and during the 12 h overnight dark phase (**B**) in  $\beta 4$ KO ( $n = 15$ ) and WT littermates ( $n = 16$ ). Post-hoc tests:  $*p < 0.05$  following Genotype  $\times$  Time interaction. **C–E**, EPM: ratio of Open arm/Total entries, percentage time spent in the open arms, percentage distance traveled in the open arms ( $\pm$ SEM), and effects of nicotine pretreatment (0.2 mg/kg) on anxiety-related response in  $\beta 4$ KO and WT mice.  $*p < 0.05$ : NaCl vs Nicotine or WT vs KO;  $***p < 0.01$ : WT vs KO. **F**, Palatable food-rewarded operant conditioning. Mean number ( $\pm$ SEM) of rewards earned during each 20 min daily sessions over the acquisition phase with 2% sucrose sweet milk (Sessions 1–12) and subsequent increase to a 10% sucrose concentration (Sessions 13–19) in  $\beta 4$ KO and WT mice (Post-hoc tests:  $*p < 0.05$ ,  $**p < 0.01$ ,  $***p < 0.001$ : compared with WT mice;  $###p < 0.001$ : Genotype main effects). **G, H**, Go/No-go task (successive discrimination procedure for a palatable food reward. H: habituation session). Mean time to enter R+ vs R– arms of a Y-maze in WT (**G**) and  $\beta 4$ KO (**H**) mice. Post-hoc tests:  $*p < 0.05$ ,  $**p < 0.01$ .  $###p = 0.005$ : Reward main effect.

$p < 0.0001$ ; Genotype:  $F_{(2,46)} = 13.30$ ,  $p = 0.001$  and Dose  $\times$  Genotype interaction:  $F_{(2,46)} = 3.62$ ,  $p = 0.035$  (Fig. 3E).

The dose–response curve (Fig. 3D) shows the mean number of self-injections for the last 3 d of the acquisition phase in WT and in KO mice. A genotype-dependent, opposite behavioral pattern was observed: nicotine intake dose-dependently decreased in WT while increasing in KO mice (two-way ANOVA, Genotype

effect:  $F_{(1,65)} = 1.47$  ns; Dose effect:  $F_{(3,65)} = 1.72$  ns; Genotype  $\times$  Dose interaction:  $F_{(3,65)} = 4.38$ ,  $p = 0.039$ ; ANOVA for Dose effect in WT:  $F_{(3,65)} = 3.87$ ,  $p = 0.018$ ). At the lowest dose (10–50 ng), KO mice did not exhibit any preference for the nicotine-reinforced arm. Conversely, at the highest dose (1200 ng), KO triggered significantly more nicotine self-injections than WT (Fig. 3D). Although the total amount of nicotine intake dose-

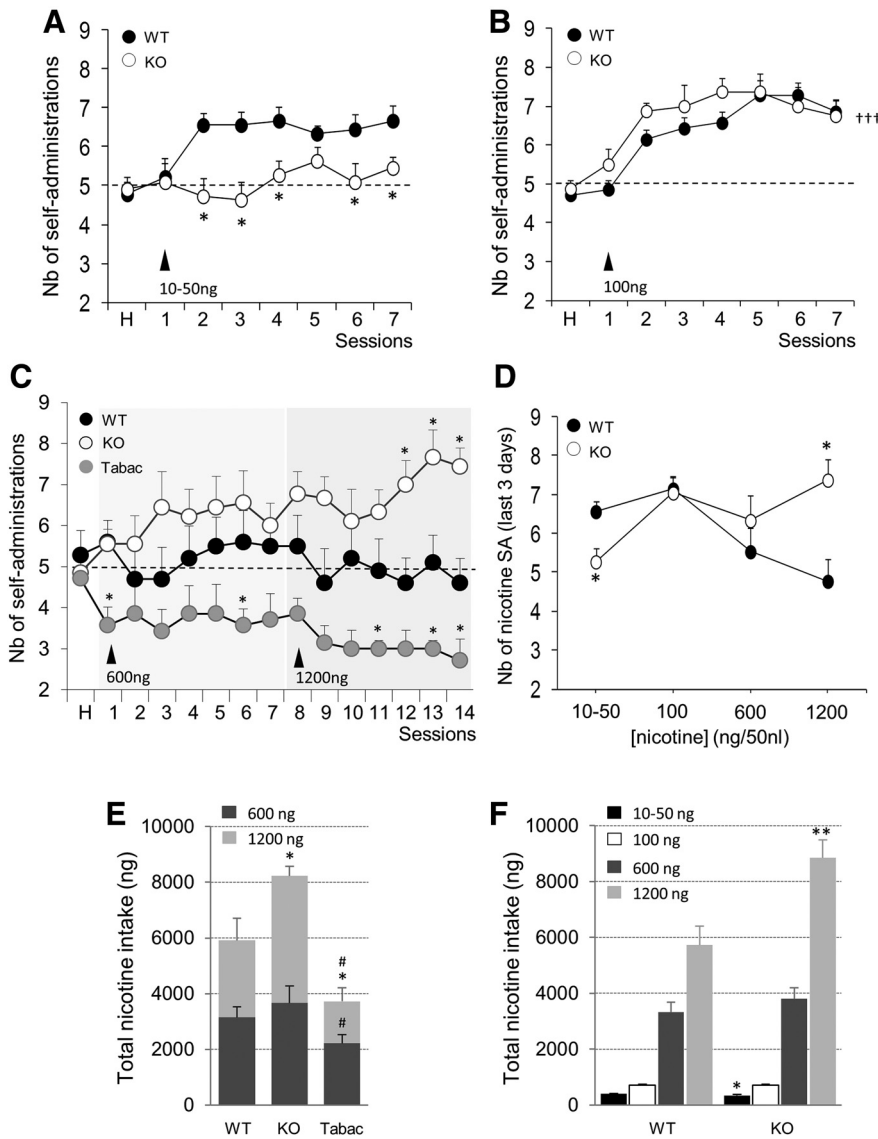


**Figure 3.** Intra-VTA nicotine self-administrations (SAs) in WT, KO and Tabac mutant mice. **A**, Mean number ( $\pm$ SEM) of SAs in WT ( $n = 9$ ) and KO ( $n = 11$ ) mice at 10–50 ng (ANOVA; Genotype effect:  $p = 0.002$ . Post-hoc tests:  $*p < 0.05$  vs WT mice). **B**, Mean number ( $\pm$ SEM) of SAs in WT ( $n = 7$ ) and KO ( $n = 8$ ) mice at the dose of 100 ng (two-way ANOVA; Session effect:  $+++p < 0.0001$ ). **C**, Mean number ( $\pm$ SEM) of SAs in WT ( $n = 10$ ), KO ( $n = 9$ ), and  $\beta 4$ -overexpressing (Tabac,  $n = 7$ ) mice at 600 ng, followed by seven sessions at 1200 ng (ANOVA for 600 ng and 1200 ng: Genotype effect;  $p = 0.039$ ,  $p = 0.001$ , respectively. Post-hoc tests:  $*p < 0.05$  vs WT mice.). **D**, Dose–response curve based on the mean number of SAs ( $\pm$ SEM) for the last 3 d of the acquisition phase according to nicotine doses in WT mice ( $n = 7–10$  per dose) and in KO mice ( $n = 8–11$  per dose). The number of self-infusions dose-dependently decreased in the WT group while increasing in KO mice.  $*p < 0.05$ : KO vs WT following Genotype  $\times$  Dose interaction and significant Dose effect in WT. **E**, Total amount of nicotine intake (ng) in WT, KO, and Tabac mice. From 600 to 1200 ng, nicotine intake steadily increased in KO while conversely decreasing significantly in Tabac to lower levels relative to WT ( $*p < 0.05$  vs WT;  $\#p < 0.05$  vs KO). At the highest dose of 1200 ng, only KO mice continue to take up to 1.3 times the maximum nicotine amount reached by WT ( $*p < 0.05$  vs WT). **F**, Total amount of nicotine intake (ng) during self-administration as measured at the end of the last three VTA-ICSA sessions for doses ranging from 10–50 to 1200 ng in WT and KO. At low to medium doses (10–50 to 100 ng), nicotine intake increased dose-dependently in both WT and  $\beta 4$ KOs, however, KO mice consumed significantly less nicotine in the low-dose range (10–50 ng:  $*p < 0.05$  vs WT). Conversely, KO consumed up to 1.5 times the amount of WT intake at 1200 ng ( $**p < 0.01$  vs WT).

dependently increased in both groups, it was lower in KO compared with WT for the lowest dose (10–50 ng; Fig. 3F); but conversely KO mice reached 1.5 times the WT level at 1200 ng (Dose effect:  $F_{(3,65)} = 11.98$ ,  $p = 0.001$ ; Genotype effect  $F_{(1,65)} = 8.70$ ,  $p = 0.044$ ; Dose  $\times$  Genotype interaction  $F_{(3,65)} = 7.41$ ,  $p = 0.007$ ). Importantly, no physical manifestations, such as scratching or shaking, were observed at any doses. Again, total intake confirmed

the genotype-dependent inverse dose–response pattern observed with the number of self-administrations (SAs).

*Overexpression of  $\beta 4^*$ nAChRs in the VTA of  $\beta 4$  KO mice increases nicotine ICSA*

We used targeted, region specific LV re-expression of the  $\beta 4$  subunit to identify the role of three  $\beta 4$ -expressing brain regions (MHb, IPN and in the VTA) in nicotine self-administration (Fig. 1A). Two groups of mice were injected with the control LV (WT-GFP<sup>VTA</sup> and KO-GFP<sup>VTA</sup>), whereas one group received the LV for  $\beta 4$  expression (KO- $\beta 4^*$ ). At the end of the last VTA-ICSA session, transduction was verified by immunofluorescent detection of GFP, and VTA expression of  $\beta 4$  was determined using autoradiographic assessment of I<sup>125</sup>-epibatidine binding sites. LV transfer of the  $\beta 4$  genetic sequence into the VTA of KO mice successfully increased A85380-resistant I<sup>125</sup>-epibatidine binding sites in this brain region (Fig. 4A). We found that  $\beta 4^*$ nAChRs level are very low or undetectable in the VTA of WT mice, therefore a quantification of relative  $\beta 4^*$ nAChR restoration was not conducted. Radioligand binding was also detected in the periphery of the neighboring IPN. Immunofluorescence analysis confirmed successful infection of the VTA, as revealed by GFP expression (Fig. 1B).

At the dose of 600 ng, both WT-GFP<sup>VTA</sup> and KO-GFP<sup>VTA</sup> mice exhibited a similar, slight preference for nicotine reminiscent of non-vectorized WT and KO mice (Fig. 4B). However, increasing the dose up to 1200 ng had an opposite effect on these two genotypes: whereas the number of nicotine SAs remained close to chance level in WT-GFP<sup>VTA</sup> or even tended to decrease, this parameter increased in KO-GFP<sup>VTA</sup> mice. WT-GFP<sup>VTA</sup> did not significantly differ from WT mice:  $F_{(1,11)} = 1.09$  ns; in contrast KO- $\beta 4^*$  exhibited a rapid increase in nicotine VTA-ICSA at the dose of 600 ng, and remained significantly higher than both WT-GFP<sup>VTA</sup> and KO-GFP<sup>VTA</sup> mice at 1200 ng. A two-way ANOVA for the 600 ng dose yielded a Genotype effect:  $F_{(2,21)} = 3.79$ ,  $p = 0.035$ ; a Session effect:  $F_{(6,126)} = 5.38$ ,  $p < 0.0001$ ; and no Genotype  $\times$  Session interaction:  $F_{(12,126)} = 1.65$  ns. At 1200 ng, Genotype effect:  $F_{(2,21)} = 24.76$ ,  $p = 0.001$ ; no Session effect:  $F_{(6,126)} = 0.5$  ns; but a Genotype  $\times$  Session interaction:  $F_{(12,126)} = 4.69$ ,  $p < 0.0001$ . As already observed in non-vectorized mice, KO-GFP<sup>VTA</sup> exhibited a higher total amount of nicotine intake

$p = 0.035$ ; a Session effect:  $F_{(6,126)} = 5.38$ ,  $p < 0.0001$ ; and no Genotype  $\times$  Session interaction:  $F_{(12,126)} = 1.65$  ns. At 1200 ng, Genotype effect:  $F_{(2,21)} = 24.76$ ,  $p = 0.001$ ; no Session effect:  $F_{(6,126)} = 0.5$  ns; but a Genotype  $\times$  Session interaction:  $F_{(12,126)} = 4.69$ ,  $p < 0.0001$ . As already observed in non-vectorized mice, KO-GFP<sup>VTA</sup> exhibited a higher total amount of nicotine intake



than WT-GFP<sup>VTA</sup> at the highest dose (1200 ng), and expression of the  $\beta 4$  subunit in the VTA of KO mice (KO- $\beta 4^{\text{VTA}}$ ) was associated with an increase in nicotine intake at both doses (Fig. 4C; Dose effect:  $F_{(1,42)} = 25.70$ ,  $p < 0.0001$ ; Genotype effect:  $F_{(2,42)} = 28.70$ ,  $p < 0.0001$ ; Dose  $\times$  Genotype interaction:  $F_{(2,42)} = 10.48$ ,  $p = 0.0002$ ). These results further support the genotype-dependent pattern revealed by analyses of the number of SAs.

#### Re-expression of $\beta 4^*$ nAChRs into either the MHb or IPN limits VTA-ICSA of high doses of nicotine

Two groups of mice were injected with the control LV (WT-GFP<sup>MHb</sup>,  $n = 6$  and KO-GFP<sup>MHb</sup>,  $n = 8$ ), and one group received the LV for  $\beta 4$  expression (KO- $\beta 4^{\text{MHb}}$ ,  $n = 6$ ) in the MHb. Targeting the MHb is challenging considering its small size and the fact that these nuclei flank the dorsal third ventricle. Therefore, levels of  $\beta 4^*$ nAChR re-expression were systematically verified among mice which completed nicotine VTA-ICSA. A85380-resistant  $I^{125}$ -epibatidine binding demonstrates that the LV successfully increases  $\beta 4^*$ nAChR binding sites in the MHb (Fig. 5A). After quantification of radiographic intensity, we identified mice with expression levels  $>30\%$  that of WT-GFP<sup>MHb</sup>, because a threshold effect of habenular  $\beta 4^*$ nAChR expression on nicotine self-administration had been identified previously (Harrington et al., 2016). The KO- $\beta 4^{\text{MHb}}$  group demonstrated a mean MHb autoradiographic intensity of 53.6% that of WT-GFP<sup>MHb</sup> controls ( $\pm 6.5\%$  SEM), which was statistically greater than levels found in KO-GFP<sup>MHb</sup> mice ( $15.0 \pm 4.2\%$ , unpaired  $t$  test:  $p < 0.0001$ ; Fig. 5A). Immunofluorescence analysis also reveals successful infection of the MHb, using GFP expression as a marker (Fig. 1B).

Expression of GFP in the MHb did not affect nicotine VTA-ICSA either in WT- or KO-GFP<sup>MHb</sup> mice, which performed similarly to their non-vectorized counterparts at both nicotine doses. In contrast, MHb re-expression of  $\beta 4^*$ nAChR restored a WT-like profile in KO- $\beta 4^{\text{MHb}}$  (Fig. 5B). Although this did not reach statistical significance at the dose of 600 ng (Genotype effect:  $F_{(2,17)} = 2.76$  ns; Session effect:  $F_{(6,102)} = 2.38$ ,  $p = 0.022$ ), raising the dose up to 1200 ng decreased nicotine choice to chance level in both WT-GFP<sup>MHb</sup> and KO- $\beta 4^{\text{MHb}}$ , whereas KO-GFP<sup>MHb</sup> continued to show a marked preference for nicotine (Genotype effect:  $F_{(2,17)} = 9.10$ ,  $p = 0.006$ ; Session effect:  $F_{(6,102)} = 1.74$  ns; Genotype  $\times$  Session interaction:  $F_{(12,102)} = 0.88$  ns). Post hoc tests confirmed that at 1200 ng, KO- $\beta 4^{\text{MHb}}$  mice followed WT-GFP<sup>MHb</sup> (KO- $\beta 4^{\text{MHb}}$  vs WT-GFP<sup>MHb</sup> ns); but differ from KO-GFP<sup>MHb</sup> (Fig. 5B).

Re-expression of  $\beta 4^*$ nAChRs in the IPN also decreases positive reinforcing effects of high doses of nicotine in  $\beta 4$ KO mice. Two groups were injected with the control LV (WT-GFP<sup>IPN</sup> and KO-GFP<sup>IPN</sup>), and one group of KO received the LV for  $\beta 4$  re-expression (KO- $\beta 4^{\text{IPN}}$ ) in the IPN. After completion of VTA-

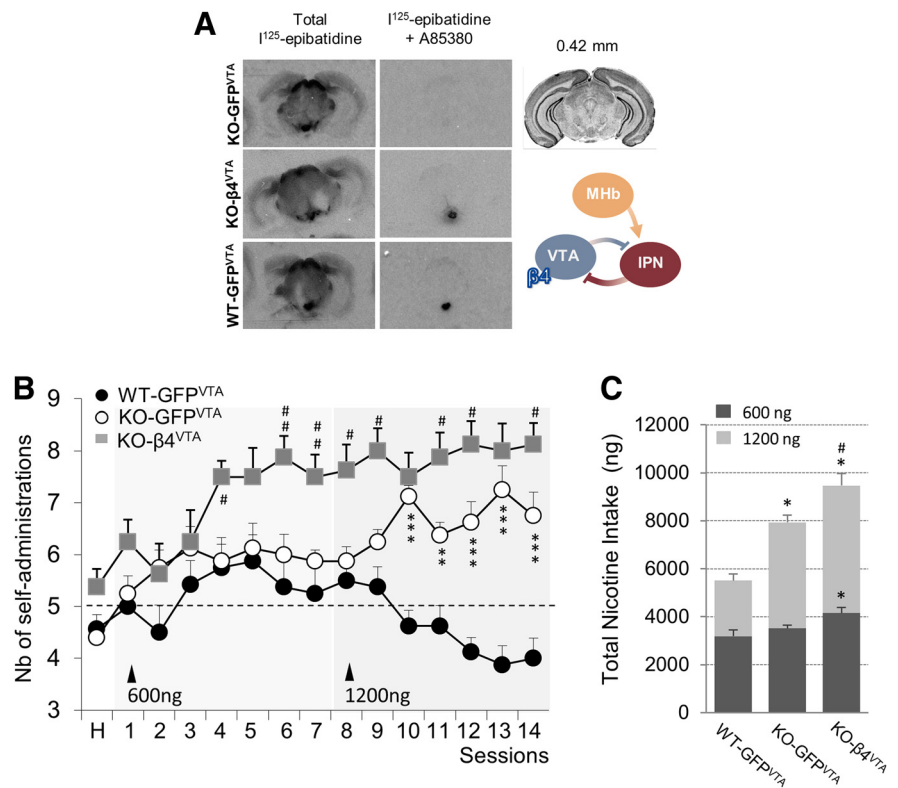


**Figure 4.** Effects of overexpression of  $\beta 4^*$ nAChRs in the VTA on nicotine VTA-ICSA. **A**, LV re-expression of  $\beta 4^*$ nAChRs in the VTA:  $I^{125}$ -staining in coronal sections of WT-GFP<sup>VTA</sup>, KO-GFP<sup>VTA</sup>, and KO- $\beta 4^{\text{VTA}}$  brains. The left column shows total  $I^{125}$ -epibatidine binding, illustrative of heteromeric nAChRs. The right column shows  $I^{125}$ -epibatidine binding of adjacent brain sections after displacement from  $\beta 2^*$ nAChR sites (A85380). AP coordinate is relative to the interaural line (Paxinos and Franklin, 2001). **B**, Mean number ( $\pm$  SEM) of intra-VTA nicotine SAs in VTA-vectorized mice (WT-GFP<sup>VTA</sup>, KO-GFP<sup>VTA</sup>, KO- $\beta 4^{\text{VTA}}$ , all groups  $n = 8$ ) at 600 and 1200 ng. ANOVA at 600 ng: Genotype and Session effects; at 1200 ng: Genotype effect. Post-hoc tests: \*\* $p < 0.01$ ; \*\*\* $p < 0.001$  (vs WT); # $p < 0.05$ , ## $p < 0.01$  (vs KO). **C**, Total amount of nicotine intake (ng) for doses ranging from 600 ng to 1200 ng in WT-GFP<sup>VTA</sup>, KO-GFP<sup>VTA</sup>, and KO- $\beta 4^{\text{VTA}}$  mice. Both KO strains exhibited increased nicotine intake compared with WT-GFP<sup>VTA</sup> at the 1200 ng dose, but this parameter was even higher in KO- $\beta 4^{\text{VTA}}$  compared with WT at the 600 ng, and also to the KO-GFP<sup>VTA</sup> at the 1200 ng dose. Post-hoc tests: \* $p < 0.05$  vs WT; # $p < 0.05$  vs KO.

ICSA, KO- $\beta 4^{\text{IPN}}$  mice were assessed for  $\beta 4^*$ nAChR expression at the site of LV delivery. Quantification of A85380-resistant  $I^{125}$ -epibatidine autoradiographic intensity shows that  $\beta 4^*$ nAChR expression is rescued to 64.2% of WT-GFP<sup>IPN</sup> controls ( $\pm 9.7\%$  SEM; Fig. 5C). Radioligand binding is almost absent in the KO-GFP<sup>IPN</sup> controls ( $2.3 \pm 0.6\%$  SEM, unpaired  $t$  test:  $p = 0.0014$ ). Immunofluorescence analysis also confirmed successful infection of the IPN, and expression of GFP (Fig. 1B).

KO-GFP<sup>IPN</sup> exhibited a dose-dependent increase in nicotine intake with a marked preference for nicotine at 1200 ng, similarly to KO mice (Fig. 5D). WT-GFP<sup>IPN</sup> displayed a WT phenotype, their performances being close to chance level throughout the VTA-ICSA experiment. IPN re-expression of  $\beta 4$  in KO mice (KO- $\beta 4^{\text{IPN}}$  mice) resulted in a sharp decrease in nicotine self-injections at both 600 and 1200 ng compared with their GFP-expressing controls, their performances becoming similar to WT-GFP<sup>IPN</sup> mice. (600 ng Genotype effect:  $F_{(2,15)} = 3.56$ ,  $p = 0.038$ ; Session effect:  $F_{(6,90)} = 1.70$  ns; Genotype  $\times$  Session interaction:  $F_{(12,90)} = 0.60$  ns; 1200 ng Genotype effect:  $F_{(2,15)} = 7.45$ ,  $p = 0.0029$ ; Session effect:  $F_{(6,90)} = 1.12$  ns; Genotype  $\times$  Session interaction:  $F_{(12,90)} = 0.87$  ns). As for their non-vectorized counterparts, KO-GFP<sup>IPN</sup> mice self-administered more nicotine than both WT-GFP<sup>IPN</sup> and KO- $\beta 4^{\text{IPN}}$  mice at 1200 ng (Fig. 5D). Analyses of total amount of nicotine intake confirmed the higher consumption of KO-GFP<sup>MHb</sup> or IPN, as already observed in non-

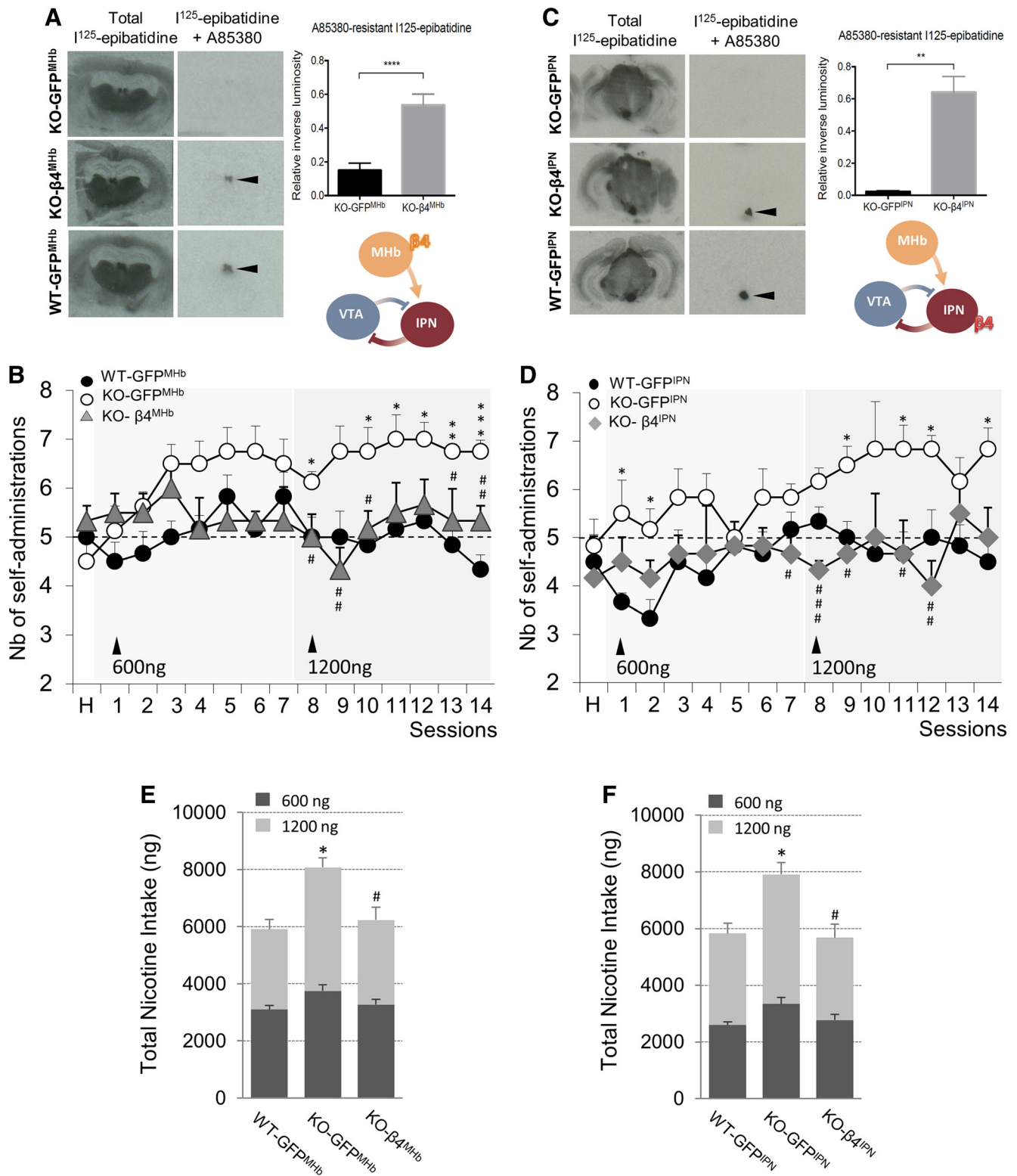


**Figure 5.** Effects of re-expression of  $\beta 4^*$ nAChRs in the Mhb-IPN pathway on nicotine VTA-ICSA. **A, C**,  $^{125}\text{I}$ -staining in coronal sections of WT-GFP<sup>Mhb</sup>, KO-GFP<sup>Mhb</sup> and KO- $\beta 4^{\text{Mhb}} brains and of WT-GFP<sup>IPN</sup>, KO-GFP<sup>IPN</sup> and KO- $\beta 4^{\text{IPN}} brains, at the level of the Mhb (**A**) and the IPN (**C**), respectively. Left columns show total  $^{125}\text{I}$ -epibatidine binding, illustrative of heteromeric nAChRs. Right columns show  $^{125}\text{I}$ -epibatidine binding of adjacent brain sections after displacement from  $\beta 2^*$ nAChR sites, revealing putative  $\beta 4^*$ nAChRs. Right panels show quantification of A85380-resistant  $^{125}\text{I}$ -epibatidine autoradiography of Mhb- and IPN-injected mice submitted to intra-VTA nicotine SA. Mean inverse luminosity of autoradiographic puncta are expressed relative to WT-GFP<sup>Mhb</sup> and WT-GFP<sup>IPN</sup> controls. ** $p < 0.01$ , **** $p < 0.0001$  (unpaired  $t$  tests). **B, D**, Mean number ( $\pm$ SEM) of intra-VTA nicotine SAs in Mhb- and IPN-vectorized mice (WT-GFP<sup>Mhb</sup> or IPN, KO-GFP<sup>Mhb</sup> or IPN, KO- $\beta 4^{\text{Mhb}} or IPN,  $n = 6-8$ ) at 600 ng and 1200 ng. Post-hoc tests: * $p < 0.05$ , ** $p < 0.01$ , *** $p < 0.001$  (vs WT) # $p < 0.05$ , ## $p < 0.01$ ; ### $p < 0.001$  (vs KO); following main effects of Genotype. **E, F**, Total amount of nicotine intake (ng) for doses ranging from 600 ng to 1200 ng in mice re-expressing the  $\beta 4$  subunit in either the Mhb (WT-GFP<sup>Mhb</sup>, KO-GFP<sup>Mhb</sup>, and KO- $\beta 4^{\text{Mhb}}) or the IPN (WT-GFP<sup>IPN</sup>, KO-GFP<sup>IPN</sup>, and KO- $\beta 4^{\text{IPN}}). LV induced re-expression of  $\beta 4$  in either the MH or the IPN led to a strikingly similar pattern of normalized, WT-like nicotine intake whatever the dose used. Post-hoc tests: * $p < 0.05$  vs WT; # $p < 0.05$  vs KO.$$$$$

vectorized and in KO-GFP<sup>VTA</sup> mice at the highest dose (1200 ng), thus providing further evidence that re-expression of  $\beta 4$  in either the MHb or IPN restored the regulation of nicotine intake to WT-GFP<sup>MHb</sup> or IPN levels (MHb, Dose effect:  $F_{(1,34)} = 162.30$ ,  $p < 0.0001$ ; Genotype effect:  $F_{(2,34)} = 11.08$ ,  $p = 0.001$ ; Dose  $\times$  Genotype interaction:  $F_{(2,34)} = 3.67$ ,  $p = 0.036$ ; IPN, Dose effect:  $F_{(1,30)} = 152.22$ ,  $p < 0.0001$ ; Genotype effect:  $F_{(2,30)} = 10.55$ ,  $p = 0.003$ ; Fig. 5E,F, respectively).

Together these results show that, despite the anatomic proximity of VTA and IPN,  $\beta 4$  over/re-expression elicited inverse responses, i.e., showing increased and decreased SA, respectively. Furthermore, analysis of different SA parameters (number of self-injections and total nicotine intake) across re-expression studies provides converging evidence that  $\beta 4^*$ nAChRs, in both the MHb and IPN, mediate a stop signal on nicotine VTA-ICSA.

## Discussion

In the present study, we characterized the implication of  $\beta 4^*$ nAChRs in anxiety- and reward-related behaviors. We report converging evidence showing that  $\beta 4$ KO exhibit severe impairments in reward processing. In the operant conditioning task for a palatable food reward, KO mice progressed over acquisition sessions and eventually learned the task, however they earned a very low number of rewards and did not increase their responses to higher sucrose concentrations compared with their WT counterparts. Food-training responses in mice undergoing intravenous self-administration procedures have not reported differences between WT and  $\beta 4$ KO (Harrington et al., 2016). However a critical factor could be that no food deprivation was used here. This may have allowed detecting a sucrose reward effect not observable under strong food deprivation. Several brain areas that express  $\beta 4$  could account for this difference. For instance  $\beta 4^*$ nAChR are present in olfactory and taste circuits (Qian et al., 2018; Spindle et al., 2018). Also viral knockdown of the  $\beta 4$  subunit in hypothalamic proopiomelanocortin neurons blocked the anorexigenic effect of cytosine, a selective agonist of  $\alpha 3\beta 4$  nAChRs (Mineur et al., 2011; Calarco et al., 2018).

To further assess motivational vs cognitive processes, we used a Go/No-go task based on a successive discrimination procedure. WT mice rapidly acquired (5–6 training days) a Go/No-go response to successive presentation of R+ and R– arms of the maze, but this behavior was not present in  $\beta 4$ KOs. Again, such an undifferentiated increase in time to reach both R+ and R– can be interpreted as a motivational deficit, whereas non-discriminating decreases in R+/R– latencies are related to impulsivity or memory impairment (Marighetto et al., 1999). Together, low reward score, insensitivity to the hedonic value of palatable foods, non-discriminating, increased latencies in the Go/No-go task and reduced nicotine self-administration all suggest that  $\beta 4$ KO mice display a blunted response to food and nicotine rewards reminiscent of a reward-deficit syndrome (Blum et al., 2000).

Response to novelty has been related to the vulnerability to develop addiction (Piazza et al., 1989).  $\beta 4$ KO mice displayed a significant increase in novelty-induced activity. Because activity during the dark phase of the cycle was similar in WT and  $\beta 4$ KOs, this cannot be considered as an alteration of motor behavior. However, exposure to an inescapable environment can elicit either an escape or an exploratory behavior, thus novelty-preference could be a more reliable predictor of vulnerability (Belin et al., 2016). We show here that  $\beta 4$ KO mice expressed a low level of anxiety in the EPM task, and were insensitive to the

anxiolytic effects of nicotine. These results are in agreement with previous studies reporting decreased anxiety-related responses and EPM-induced and heart rate in  $\beta 4$ KO mice (Picciotto et al., 2002; Salas et al., 2003; Semenova et al., 2012; Ables et al., 2017; Wolfman et al., 2018). It would be interesting to dissect which brain area expressing  $\beta 4^*$ nAChRs is implicated in this trait.

We used a mouse model of ICSA to investigate the reactivity of the reward system by injecting nicotine directly into the VTA. This procedure is a powerful paradigm to assess positive reinforcing/aversive properties of drugs of abuse, an interesting feature when using substances considered sometimes as low reinforcers such as nicotine (Maskos et al., 2005; Besson et al., 2006; David et al., 2006; Exley et al., 2011). Extensive evidence supports the view that acute reinforcing properties of drugs of abuse play a critical role in the early stages of the addiction cycle, in particular for drug-related habits and possibly relapse (Wise and Koob, 2014). In agreement with the reduced nicotine IVSA observed in  $\beta 4$ KO mice (Harrington et al., 2016), we found a decrease in nicotine VTA-ICSA at low to moderate doses. Concurrent nicotine delivery and electrophysiological measurements in the same brain area was not technically feasible, but previous work has provided valuable information on nicotine-induced activity of VTA-DA cells in  $\beta 4$ KO mice (Harrington et al., 2016). Although a slight increase in the sensitivity of VTA-DA neurons to IV nicotine in KO mice compared with WT group was observed at the lowest dose, nicotine-induced bursting and more specifically the number of spikes within burst, a parameter closely related to reinforcing properties (Tolu et al., 2013), was significantly reduced in  $\beta 4$ KOs.

When increasing the nicotine dose up to 10 times the threshold, KO mice exhibited SA levels similar to WT. The difference in responding to high nicotine doses when using IVSA vs ICSA could be due to the recruitment of systemic/autonomic nAChRs when using IVSA. Indeed, one of the most interesting findings of the current study is the converging evidence provided by two parameters (number of self-injections and total amount of nicotine intake) indicating that self-limitation processes normally occurring at the highest doses in WT, are altered in  $\beta 4$ KO mice. By focusing on the reward system, VTA-ICSA allows to explore the effects of high doses, an interesting prospect with regards to the relationship between human genetic variants in the *CHRNA5-A3-B4* locus and heavy smoking (Thorgeirsson et al., 2008; Weiss et al., 2008). Direct comparison of brain nicotine concentrations achieved in rodents and humans is difficult, mainly because of differences in routes of administration and related pharmacokinetics. Following one cigarette (or 10 puffs), brain nicotine concentration has been estimated between 0.5 and 1  $\mu\text{M}$  (Rose et al., 2010). We observed nicotine VTA-ICSA at concentrations starting from 10 to 100  $\mu\text{M}$  in WT mice. The ED<sub>50</sub> for ACh or nicotine-induced activation of nAChRs are very similar and depend on the receptor subtype and affinity, ranging from 70 to 200  $\mu\text{M}$  for  $\alpha 4\beta 2^*$  and  $\alpha 7^*$ nAChRs, respectively, and both synaptic ACh release and nicotine-evoked currents peak at millimolar concentrations (Buisson and Bertrand, 2001). Interestingly, in habitual smokers the absence of puff-associated oscillations (spikes) in brain nicotine concentration suggests that heavy smoking could be more related to the progressive increase in nicotine concentration (Rose et al., 2010). While  $\beta 4$ KO mice dose-dependently increased their nicotine intake up to the millimolar range, VTA-ICSA decreased at higher doses in WT mice and  $\beta 4$  overexpressing Tabac mice learned to avoid nicotine, choosing the non-reinforced arm in 75% of trials. The opposite pattern of  $\beta 4$ KO and Tabac mice suggests that nicotine intake is

inversely related to the amount of functional  $\beta 4$  subunits. These observations are consistent with previous reports suggesting an implication of these receptors in nicotine's aversive effects (Fowler and Kenny, 2014; Antolin-Fontes et al., 2015). However, Tabac mice express  $\beta 4^*$ nAChRs also in brain regions that show nondetectable levels in WT mice, such as amygdala, substantia nigra, and supra-mammillary nuclei (Frahm et al., 2011), that could contribute to the aversion to nicotine shown in these mice.

Because VTA re-expression of the  $\beta 4$  subunit in KO mice produced neither a WT nor a Tabac phenotype, we attribute the self-regulation of nicotine intake at high doses to extra-VTA  $\beta 4^*$ nAChRs. Re-expression of the  $\beta 4$  subunit in either the MHb or IPN restored self-limitation effects toward a WT-like phenotype. Despite the adjacent localization of IPN with the VTA and likely stimulation of both VTA and IPN nAChRs by intra-VTA nicotine, we observed opposite effects of IPN (decrease) and VTA (increase) re-expression of  $\beta 4$  on nicotine VTA-ICSA. Because  $\beta 4^*$ nAChR expression was very low or even undetectable in the VTA of WT mice (Gahring et al., 2004; Yang et al., 2009; Baddick and Marks, 2011), reward facilitating effects could be related to an overexpression of VTA  $\beta 4$  subunits, or ectopic expression in neuronal subpopulations of the VTA. Therefore, it is difficult to infer the physiological role of VTA  $\beta 4^*$ nAChRs from the re-expression study. Yet, restoration of a self-limited nicotine intake through MHb or IPN re-expression suggests that the alteration of the MHb-IPN-negative feedback control in  $\beta 4$ KO mice may have promoted a “go” signal for high doses of nicotine. Thus, MHb-IPN  $\beta 4^*$ nAChRs appear to mediate an ACh-dependent stop signal. In agreement with this view, lidocaine-induced inactivation of either MHb or IPN increases nicotine IVSA in the rat, whereas lentiviral overexpression of  $\beta 4$  subunit in the MHb decreases nicotine consumption in the two-bottle drinking test (Fowler et al., 2011; Slimak et al., 2014). Notably, our results suggest an implication of  $\beta 4^*$ nAChRs in a “satiety-like” signal limiting nicotine VTA-ICSA, rather than aversion per se. As reported here for the  $\beta 4$  subunit, re-expression of the  $\alpha 5$  subunit in the MHb of  $\alpha 5$ KO mice reduced aberrant SA of high doses of nicotine, whereas MHb-specific knockdown of this subunit in rats mimics the increase in nicotine intake of  $\alpha 5$ KO mice (Fowler et al., 2011). Consistently, viral-induced expression of an allelic variant of *CHRNA5* ( $\alpha 5D398N$ ) found in heavy smokers, in the MHb of Tabac mice, restored nicotine intake to WT levels (Frahm et al., 2011). Therefore, there are striking similarities in the SA phenotype of  $\alpha 5$  and  $\beta 4$ -null mutants as reported here. Interestingly, levels of  $\alpha 5$  (more in VTA and few in MHb) and  $\beta 4$  subunit expression (low in VTA and dense in MHb) are inverted in WT (Hsu et al., 2013, 2014). Understanding their respective role in emotional regulation could help to develop new therapeutic interventions against tobacco dependence.

The demonstration that  $\beta 4^*$ nAChRs act outside of the VTA to limit ICSA of high nicotine doses raises a question regarding the endogenous cholinergic stimulation of  $\beta 4^*$ nAChRs. The septum is an appealing target, because it receives a DAergic input from the VTA and sends a cholinergic output to the MHb (Contestabile and Fonnum, 1983; Sperlagh et al., 1998). Inhibition of VTA-D1 dopamine receptors blocks the rewarding effects of intraseptal GABA(A) agonists (Gavello-Baudy et al., 2008), and selective elimination of the dorsal septo-habenular pathway results in aversive learning deficits (Yamaguchi et al., 2013). Further research is required to investigate the role of the meso-septo-habenular circuit in the reward/aversion balance, and how this information is relayed from the MHb-IPN pathway to the VTA. To

date, there is evidence for direct influences through MHb- or IPN-VTA connections (Sutherland, 1982), or indirectly through IPN-dependent modulation of the dorsal raphe nucleus (Hsu et al., 2013, 2014) or through IPN-laterodorsal tegmentum projections (Ables et al., 2017; Wolfman et al., 2018). Although  $\alpha 5^*$ nAChRs presynaptically modulate glutamate and noradrenaline release in the IPN, only  $\beta 4^*$ nAChRs stimulate IPN ACh release (Grady et al., 2009; Beiranvand et al., 2014). In the present study, nicotine infusions were restricted to the VTA, thus raising an important question about the relevance of this ACh-dependent negative feedback mechanism in smokers. Chronic nicotine upregulates nAChRs in rodent and human brain and sensitizes the MHb-IPN pathway (Marks et al., 1992; Mamede et al., 2007; Arvin et al., 2019). The behavioral consequences of this sensitization are not fully understood, and it is unclear whether direct effects of nicotine on this circuit and/or chronic treatment are necessary (Görllich et al., 2013). Optogenetic stimulation and nicotine are equally effective in priming aversion through activation of IPN GABAergic neurons (Morton et al., 2018). Here we report that VTA nicotine infusions elicit a  $\beta 4$ , MHb/IPN-mediated negative feedback regulating intake. Therefore, any alteration of the  $\beta 4^*$ nAChR function could result in a dampened self-limiting signal. Importantly, if not strictly nicotine-dependent, this endogenous ACh  $\beta 4$ -mediated mechanism could be relevant for other drugs of abuse as well, thus accounting for the implication of *CHRNA3/A5/B4* cluster variants in the risk of dependence on multiple substances (Sherva et al., 2010). Similar regulatory effects of MHb and IPN  $\beta 4^*$ nAChRs stimulation on nicotine VTA-ICSA are also consistent with a feedback inhibition of MHb by IPN neurons (Ables et al., 2017). How ACh, and other neurotransmitters in the Hb-IPN, regulate positive/negative motivational signals is a critical question for future research.

In conclusion, we demonstrate that lack of functional  $\beta 4^*$ nAChRs results in an addiction-related phenotype characterized by decreased anxiety, severe impairments in reward-guided behaviors, decreased nicotine SA at low to moderate doses, but increased nicotine intake at doses eliciting self-limitation in WT animals. LV-induced re-expression of the  $\beta 4$  subunit into either the MHb or IPN restored the self-limiting signal on nicotine SA, suggesting that activation of  $\beta 4^*$ nAChRs in the MHb-IPN axis exerts a negative control on central nicotine reward.

## References

- Ables JL, Görllich A, Antolin-Fontes B, Wang C, Lipford SM, Riad MH, Ren J, Hu F, Luo M, Kenny PJ, Heintz N, Ibañez-Tallon I (2017) Retrograde inhibition by a specific subset of interpeduncular  $\alpha 5$  nicotinic neurons regulates nicotine preference. *Proc Natl Acad Sci U S A* 114:13012–13017.
- Amos CI, Wu X, Broderick P, Gorlov IP, Gu J, Eisen T, Dong Q, Zhang Q, Gu X, Vijayakrishnan J, Sullivan K, Matakidou A, Wang Y, Mills G, Doheny K, Tsai YY, Chen WV, Shete S, Spitz MR, Houlston RS (2008) Genome-wide association scan of tag SNPs identifies a susceptibility locus for lung cancer at 15q25.1. *Nat Genet* 40:616–622.
- Antolin-Fontes B, Ables JL, Görllich A, Ibañez-Tallon I (2015) The habenulo-interpeduncular pathway in nicotine aversion and withdrawal. *Neuropharmacology* 96:213–222.
- Arvin MC, Jin XT, Yan Y, Wang Y, Ramsey MD, Kim VJ, Beckley NA, Henry BA, Drenan RM (2019) Chronic nicotine exposure alters the neurophysiology of habenulo-interpeduncular circuitry. *J Neurosci* 39:4268–4281.
- Azam L, Winzer-Serhan UH, Chen Y, Leslie FM (2002) Expression of neuronal nicotinic acetylcholine receptor subunit mRNAs within midbrain dopamine neurons. *J Comp Neur* 444:260–274.
- Baddick CG, Marks MJ (2011) An autoradiographic survey of mouse brain nicotinic acetylcholine receptors defined by null mutants. *Biochem Pharmacol* 82:828–841.

- Baudonnat M, Guillou JL, Husson M, Vandesquille M, Corio M, Decorte L, Faugère A, Porte Y, Mons N, David V (2011) Disrupting effect of drug-induced reward on spatial but not cue-guided learning: implication of the striatal protein kinase A/cAMP response element-binding protein pathway. *J Neurosci* 31:16517–16528.
- Beiranvand F, Zlabinger C, Orr-Urtreger A, Ristel R, Huck S, Scholze P (2014) Nicotinic acetylcholine receptors control acetylcholine and noradrenaline release in the rodent habenulo-interpeduncular complex. *Br J Pharmacol* 171:5209–5224.
- Belin D, Belin-Rauscent A, Everitt BJ, Dalley JW (2016) In search of predictive endophenotypes in addiction: insights from preclinical research. *Genes Brain Behav* 15:74–88.
- Besson M, David V, Suarez S, Cormier A, Cazala P, Changeux JP, Granon S (2006) Genetic dissociation of two behaviors associated with nicotine addiction: beta-2 containing nicotinic receptors are involved in nicotine reinforcement but not in withdrawal syndrome. *Psychopharmacology* 187:189–199.
- Blum K, Braverman ER, Holder JM, Lubar JF, Monastra VJ, Miller D, Lubar JO, Chen TJ, Comings DE (2000) Reward deficiency syndrome: a biogenetic model for the diagnosis and treatment of impulsive, addictive, and compulsive behaviors. *J Psychoactive Drugs* 32:1–112.
- Buisson B, Bertrand D (2001) Chronic exposure to nicotine upregulates the human  $\alpha 4\beta 2$  nicotinic acetylcholine receptor function. *J Neurosci* 21:1819–1829.
- Calarco CA, Li Z, Taylor SR, Lee S, Zhou W, Friedman JM, Mineur YS, Gotti C, Picciotto MR (2018) Molecular and cellular characterization of nicotinic acetylcholine receptor subtypes in the arcuate nucleus of the mouse hypothalamus. *Eur J Neurosci* 48:1600–1619.
- Changeux JP (2010) Nicotine addiction and nicotinic receptors: lessons from genetically modified mice. *Nat Rev Neurosci* 11:389–401.
- Cho YH, Jeantet Y (2010) Differential involvement of prefrontal cortex, striatum, and hippocampus in DRL performance in mice. *Neurobiol Learn Mem* 93:85–91.
- Contestabile A, Fonnum F (1983) Cholinergic and GABAergic forebrain projections to the habenula and nucleus interpeduncularis: surgical and kainic acid lesions. *Brain Res* 275:287–297.
- David V, Besson M, Changeux JP, Granon S, Cazala P (2006) Reinforcing effects of nicotine microinjections into the ventral tegmental area of mice: dependence on cholinergic nicotinic and dopaminergic D1 receptors. *Neuropharmacology* 50:1030–1040.
- Exley R, Maubourguet N, David V, Eddine R, Evrard A, Pons S, Marti F, Threlfell S, Cazala P, McIntosh JM, Changeux JP, Maskos U, Cragg SJ, Faure P (2011) Distinct contributions of nicotinic acetylcholine receptor subunit alpha4 and subunit alpha6 to the reinforcing effects of nicotine. *Proc Natl Acad Sci U S A* 108:7577–7582.
- Fowler CD, Kenny PJ (2014) Nicotine aversion: neurobiological mechanisms and relevance to tobacco dependence vulnerability. *Neuropharmacology* 76:533–544.
- Fowler CD, Lu Q, Johnson PM, Marks MJ, Kenny PJ (2011) Habenular alpha5 nicotinic receptor subunit signalling controls nicotine intake. *Nature* 471:597–601.
- Frahm S, Slimak MA, Ferrarese L, Santos-Torres J, Antolin-Fontes B, Auer S, Filkin S, Pons S, Fontaine JF, Tsetlin V, Maskos U, Ibañez-Tallon I (2011) Aversion to nicotine is regulated by the balanced activity of beta4 and alpha5 nicotinic receptor subunits in the medial habenula. *Neuron* 70:522–535.
- Gahring LC, Persiyonov K, Rogers SW (2004) Neuronal and astrocyte expression of nicotinic receptor subunit beta4 in the adult mouse brain. *J Comp Neurol* 468:322–333.
- Gallego X, Molas S, Amador-Arjona A, Marks MJ, Robles N, Murtra P, Armengol L, Fernández-Montes RD, Gratacòs M, Pumarola M, Cabrera R, Maldonado R, Sabrià J, Estivill X, Dierssen M (2012) Overexpression of the CHRNA5/A3/B4 genomic cluster in mice increases the sensitivity to nicotine and modifies its reinforcing effects. *Amino acids* 43:897–909.
- Gavello-Baudy S, Le Merrer J, Decorte L, David V, Cazala P (2008) Self-administration of the GABAA agonist muscimol into the medial septum: dependence on dopaminergic mechanisms. *Psychopharmacology* 201:219–228.
- Glick SD, Ramirez RL, Livi JM, Maisonneuve IM (2006) 18-Methoxycoronaridine acts in the medial habenula and/or interpeduncular nucleus to decrease morphine self-administration in rats. *Eur J Pharmacol* 537:94–98.
- Görlich A, Antolin-Fontes B, Ables JL, Frahm S, Slimak MA, Dougherty JD, Ibañez-Tallon I (2013) Reexposure to nicotine during withdrawal increases the pacemaking activity of cholinergic habenular neurons. *Proc Natl Acad Sci U S A* 110:17077–17082.
- Gotti C, Clementi F, Fornari A, Gaimarri A, Guiducci S, Manfredi I, Moretti M, Pedrazzi P, Pucci L, Zoli M (2009) Structural and functional diversity of native brain neuronal nicotinic receptors. *Biochem Pharmacol* 78:703–711.
- Grady SR, Moretti M, Zoli M, Marks MJ, Zanardi A, Pucci L, Clementi F, Gotti C (2009) Rodent habenulo-interpeduncular pathway expresses a large variety of uncommon nAChR subtypes, but only the  $\alpha 3\beta 4^*$  and  $\alpha 3\beta 3\beta 4^*$  subtypes mediate acetylcholine release. *J Neurosci* 29:2272–2282.
- Harrington L, Vinals X, Herrera-Solis A, Flores A, Morel C, Tolu S, Faure P, Maldonado R, Maskos U, Robledo P (2016) Role of  $\beta 4^*$  nicotinic acetylcholine receptors in the habenulo-interpeduncular pathway in nicotine reinforcement in mice. *Neuropsychopharmacology* 41:1790–1802.
- Hartmann-Boyce J, Stead LF, Cahill K, Lancaster T (2013) Efficacy of interventions to combat tobacco addiction: cochrane update of 2012 reviews. *Addiction* 108:1711–1721.
- Hsu YW, Tempest L, Quina LA, Wei AD, Zeng H, Turner EE (2013) Medial habenula output circuit mediated by  $\alpha 5$  nicotinic receptor-expressing GABAergic neurons in the interpeduncular nucleus. *J Neurosci* 33:18022–18035.
- Hsu YW, Wang SD, Wang S, Morton G, Zariwala HA, de la Iglesia HO, Turner EE (2014) Role of the dorsal medial habenula in the regulation of voluntary activity, motor function, hedonic state, and primary reinforcement. *J Neurosci* 34:11366–11384.
- Jackson KJ, Martin BR, Changeux JP, Damaj MI (2008) Differential role of nicotinic acetylcholine receptor subunits in physical and affective nicotine withdrawal signs. *J Pharmacol Exp Ther* 325:302–312.
- Klink R, de Kerchove d'Exaerde A, Zoli M, Changeux JP (2001) Molecular and physiological diversity of nicotinic acetylcholine receptors in the midbrain dopaminergic nuclei. *J Neurosci* 21:1452–1463.
- Mamede M, Ishizu K, Ueda M, Mukai T, Iida Y, Kawashima H, Fukuyama H, Togashi K, Saji H (2007) Temporal change in human nicotinic acetylcholine receptor after smoking cessation: 5IA SPECT study. *J Nucl Med* 48:1829–1835.
- Marighetto A, Etchamendy N, Touzani K, Torrea CC, Yee BK, Rawlins JN, Jaffard R (1999) Knowing which and knowing what: a potential mouse model for age-related human declarative memory decline. *Eur J Neurosci* 11:3312–3322.
- Marks MJ, Pauly JR, Gross SD, Deneris ES, Hermans-Borgmeyer I, Heinemann SF, Collins AC (1992) Nicotine binding and nicotinic receptor subunit RNA after chronic nicotine treatment. *J Neurosci* 12:2765–2784.
- Maskos U, Molles BE, Pons S, Besson M, Guiard BP, Guilloux JP, Evrard A, Cazala P, Cormier A, Mameli-Engvall M, Dufour N, Cloez-Tayarani I, Bemelmans AP, Mallet J, Gardier AM, David V, Faure P, Granon S, Changeux JP (2005) Nicotine reinforcement and cognition restored by targeted expression of nicotinic receptors. *Nature* 436:103–107.
- McCallum SE, Cowe MA, Lewis SW, Glick SD (2012)  $\alpha 3\beta 4$  nicotinic acetylcholine receptors in the medial habenula modulate the mesolimbic dopaminergic response to acute nicotine *in vivo*. *Neuropharmacology* 63:434–440.
- McGehee DS, Role LW (1995) Physiological diversity of nicotinic acetylcholine receptors expressed by vertebrate neurons. *Annu Rev Physiol* 57:521–546.
- Mineur YS, Abizaid A, Rao Y, Salas R, DiLeone RJ, Gundisch D, Diano S, De Biasi M, Horvath TL, Gao XB, Picciotto MR (2011) Nicotine decreases food intake through activation of POMC neurons. *Science* 332:1330–1332.
- Morton G, Nasirova N, Sparks DW, Brodsky M, Sivakumaran S, Lambe EK, Turner EE (2018) ChRNA5-expressing neurons in the interpeduncular nucleus mediate aversion primed by prior stimulation or nicotine exposure. *J Neurosci* 38:6900–6920.
- Paxinos G, Franklin KBJ (2001) *The Mouse Brain in Stereotaxic Coordinates*. Academic Press: San Diego.
- Piazza PV, Deminière JM, Le Moal M, Simon H (1989) Factors that predict individual vulnerability to amphetamine self-administration. *Science* 245:1511–1513.

- Picciotto MR, Mineur YS (2014) Molecules and circuits involved in nicotine addiction: the many faces of smoking. *Neuropharmacology* 76:545–553.
- Picciotto MR, Brunzell DH, Caldarone BJ (2002) Effect of nicotine and nicotinic receptors on anxiety and depression. *Neuroreport* 13:1097–1106.
- Qian J, Mummalaneni S, Grider JR, Damaj MI, Lyall V (2018) Nicotinic acetylcholine receptors (nAChRs) are expressed in Trpm5 positive taste receptor cells (TRCs). *PLoS One* 13:e0190465.
- Rose JE, Mukhin AG, Lokitz SJ, Turkington TG, Herskovic J, Behm FM, Garg S, Garg PK (2010) Kinetics of brain nicotine accumulation in dependent and nondependent smokers assessed with PET and cigarettes containing 11C-nicotine. *Proc Natl Acad Sci U S A* 107:5190–5195.
- Sacone NL, Wang JC, Breslau N, Johnson EO, Hatsukami D, Saccone SF, Gruzca RA, Sun L, Duan W, Budde J, Culverhouse RC, Fox L, Hinrichs AL, Steinbach JH, Wu M, Rice JP, Goate AM, Bierut LJ (2009) The CHRNA5-CHRNA3-CHRNA4 nicotinic receptor subunit gene cluster affects risk for nicotine dependence in African-Americans and in European-Americans. *Cancer Res* 69:6848–6856.
- Salas R, Pieri F, De BM (2004a) Decreased signs of nicotine withdrawal in mice null for the  $\beta 4$  nicotinic acetylcholine receptor subunit. *J Neurosci* 24:10035–10039.
- Salas R, Cook KD, Bassetto L, De Biasi M (2004b) The  $\alpha 3$  and  $\beta 4$  nicotinic acetylcholine receptor subunits are necessary for nicotine-induced seizures and hypolocomotion in mice. *Neuropharmacology* 47:401–407.
- Salas R, Sturm R, Boulter J, De Biasi M (2009) Nicotinic receptors in the habenulo-interpeduncular system are necessary for nicotine withdrawal in mice. *J Neurosci* 29:3014–3018.
- Salas R, Pieri F, Fung B, Dani JA, De Biasi M (2003) Altered anxiety-related responses in mutant mice lacking the  $\beta 4$  subunit of the nicotinic receptor. *J Neurosci* 23:6255–6263.
- Semenova S, Contet C, Roberts AJ, Markou A (2012) Mice lacking the beta4 subunit of the nicotinic acetylcholine receptor show memory deficits, altered anxiety- and depression-like behavior, and diminished nicotine-induced analgesia. *Nicotine Tob Res* 14:1346–1355.
- Sherva R, Kranzler HR, Yu Y, Logue MW, Poling J, Arias AJ, Anton RF, Oslin D, Farrer LA, Gelernter J (2010) Variation in nicotinic acetylcholine receptor genes is associated with multiple substance dependence phenotypes. *Neuropsychopharmacology* 35:1921–1931.
- Shih PY, Engle SE, Oh G, Deshpande P, Puskar NL, Lester HA, Drenan RM (2014) Differential expression and function of nicotinic acetylcholine receptors in subdivisions of medial habenula. *J Neurosci* 34:9789–9802.
- Slimak MA, Ables JL, Frahm S, Antolin-Fontes B, Santos-Torres J, Moretti M, Gotti C, Ibañez-Tallon I (2014) Habenular expression of rare missense variants of the  $\beta 4$  nicotinic receptor subunit alters nicotine consumption. *Front Hum Neurosci* 8:12.
- Sperlagh B, Magloczky Z, Vizi ES, Freund TF (1998) The triangular septal nucleus as the major source of ATP release in the rat habenula: a combined neurochemical and morphological study. *Neuroscience* 86:1195–1207.
- Spindle MS, Parsa PV, Bowles SG, D'Souza RD, Vijayaraghavan S (2018) A dominant role for the beta 4 nicotinic receptor subunit in nicotinic modulation of glomerular microcircuits in the mouse olfactory bulb. *J Neurophysiol* 120:2036–2048.
- Sutherland RJ (1982) The dorsal diencephalic conduction system: a review of the anatomy and functions of the habenular complex. *Neurosci Biobehav Rev* 6:1–13.
- Thorgeirsson TE, Geller F, Sulem P, Rafnar T, Wiste A, Magnusson KP, Manolescu A, Thorleifsson G, Stefansson H, Ingason A, Stacey SN, Bergthorsson JT, Thorlacius S, Gudmundsson J, Jonsson T, Jakobsdottir M, Saemundsdottir J, Olafsdottir O, Gudmundsson LJ, Bjornsdottir G, et al. (2008) A variant associated with nicotine dependence, lung cancer and peripheral arterial disease. *Nature* 452:638–642.
- Tolu S, Eddine R, Marti F, David V, Graupner M, Pons S, Baudonnat M, Husson M, Besson M, Reperant C, Zemdegs J, Pages C, Hay YA, Lambollez B, Caboche J, Gutkin B, Gardier AM, Changeux JP, Faure P, Maskos U (2013) Co-activation of VTA DA and GABA neurons mediates nicotine reinforcement. *Mol Psychiatry* 18:382–393.
- Velasquez KM, Molfese DL, Salas R (2014) The role of the habenula in drug addiction. *Front Hum Neurosci* 8:174.
- Weiss RB, Baker TB, Cannon DS, von Niederhausen A, Dunn DM, Matsunami N, Singh NA, Baird L, Coon H, McMahon WM, Piper ME, Fiore MC, Scholand MB, Connett JE, Kanner RE, Gahring LC, Rogers SW, Hoidal JR, Leppert MF (2008) A candidate gene approach identifies the CHRNA5-A3-B4 region as a risk factor for age-dependent nicotine addiction. *PLoS Genet* 4:e1000125.
- WHO (2011) Report on the Global Tobacco Epidemic, 2011: warning about the dangers of tobacco. [http://www.who.int/gate1.inist.fr/tobacco/global\\_report/2011/en](http://www.who.int/gate1.inist.fr/tobacco/global_report/2011/en).
- Wise RA, Koob GF (2014) The development and maintenance of drug addiction. *Neuropsychopharmacology* 39:254–262.
- Wolfman SL, Gill DF, Bogdanic F, Long K, Al-Hasani R, McCall JG, Bruchas MR, McGehee DS (2018) Nicotine aversion is mediated by GABAergic interpeduncular nucleus inputs to laterodorsal tegmentum. *Nat Commun* 9:2710.
- Yamaguchi T, Danjo T, Pastan I, Hikida T, Nakanishi S (2013) Distinct roles of segregated transmission of the septo-habenular pathway in anxiety and fear. *Neuron* 78:537–544.
- Yang K, Hu J, Lucero L, Liu Q, Zheng C, Zhen X, Jin G, Lukas RJ, Wu J (2009) Distinctive nicotinic acetylcholine receptor functional phenotypes of rat ventral tegmental area dopaminergic neurons. *J Physiol* 587:345–361.
- Zoli M, Le Novère N, Hill JA Jr, Changeux JP (1995) Developmental regulation of nicotinic ACh receptor subunit mRNAs in the rat central and peripheral nervous systems. *J Neurosci* 15:1912–1939.